



Article



Gaseous and Particulate Matter Emissions and Dispersion from Aircraft Activities at the Copenhagen Airport

Mihalis Lazaridis^{1,*}, Eleftheria Chalvatzaki¹, Markus Bittermann², Paul Gebhardt² and Sofia Eirini Chatoutsidou¹

¹ School of Chemical and Environmental Engineering, Technical University of Crete, 73100 Chania, Greece

² Faculty of Civil and Environmental Engineering, Vienna University of Technology, Karlsplatz 13/249-01, 1040 Vienna, Austria

* Correspondence: mlazaridis@tuc.gr; Tel.: +30-28210-06172

How To Cite: Lazaridis, M., Chalvatzaki, E., Bittermann, M., et al. Gaseous and particulate matter emissions and dispersion from aircraft activities at the Copenhagen airport. *Environmental Contamination: Causes and Solutions* 2026, 2(1), 3. <https://doi.org/10.53941/eccs.2026.100003>

Received: 18 March 2026

Revised: 14 May 2026

Accepted: 27 May 2026

Published: 4 June 2026

Abstract: Emissions of four pollutants (NO_x, CO, particle mass (PM), and ultrafine particles (UFPs)) were estimated during aircraft activity at Copenhagen airport. The emissions were estimated for 5 discrete aircraft phases (taxi out, taxi in, take off, climb out, approach/landing) as well as Auxiliary Power Units (APUs) and handling which remain insufficiently characterized in the scientific literature. A Gaussian dispersion model (ISC3-ST) was applied to obtain pollutant dispersion in the vicinity of the airport. Dispersion models are widely used to simulate pollutant concentrations at various airports with most studies dealing with criteria pollutants (NO_x, CO, PM). This study evaluated the impact from aviation activities including an emerging pollutant like UFPs. Besides criteria pollutants, assessing the UFPs concentrations at ground level and in the vicinity of airports is critical for evaluating human exposure. Numerical simulations showed that elevated NO_x concentrations exceeded the regulated hourly values in the vicinity of the airport facilities. High UFPs concentrations were also modelled close to the airport with daily average values at 100,000 particles/cm³ at the airfield area and values close to 10,000 particles/cm³ at distances close to one kilometer downwind from the airport. Contrary, reduced contribution from aircraft LTO cycles to the ground-level CO and PM was found, with concentrations being lower than the air quality threshold values. These results underline that NO_x and UFPs are significant contributors to exposure for both airport workers and residents living close to the airport while CO and PM are more relevant only for the former.

Keywords: airport; emissions; concentration; dispersion model; ultrafine particles; Copenhagen

1. Introduction

Emissions of anthropogenic gaseous air pollutants and particles in urban areas have been associated with human health effects [1–3]. The transport sector is a major contributor to air pollution including on-road and non-road traffic. Emissions arising from airport activities pose a major concern to public health due to exposure to gaseous pollutants (e.g., NO₂, CO), airborne particle mass (PM), black carbon (BC), polycyclic aromatic hydrocarbons (PAHs) and particle number (PN) [4–11]. Major aviation activities are related to main aircraft engines, APU's (Auxiliary Power Units) and handling equipment. Elevated levels of NO₂ and ultrafine particles (UFP) have been measured in a number of airports [12–15] as well increased levels of hydrocarbons and CO [16]. Assessing the effects from aviation emissions on human health on a global scale has shown a considerable impact of fine particles to mortality in an area within 20 km from the airports [17].



Copyright: © 2026 by the authors. This is an open access article under the terms and conditions of the Creative Commons Attribution (CC BY) license (<https://creativecommons.org/licenses/by/4.0/>).

Publisher's Note: Scilight stays neutral with regard to jurisdictional claims in published maps and institutional affiliations.

Numerical studies using the American Meteorological Society/Environmental Protection Agency Regulatory Model (AERMOD) model have been performed in a number of airports revealing high NO₂ concentrations in the area close to the airport which exceeded the air quality limit values [7,18–20]. A Gaussian model was also used to determine the dispersion of air pollutants from aircrafts [9] and the impact of future climatic scenarios on local air quality [21]. Moreover, Voogt et al. [22] studied the use of ultrafine particle concentrations arising from aviation emission for epidemiological analysis.

The current work, focuses on estimating airport emissions of gaseous pollutants and particles from the Copenhagen airport, Denmark and their environmental impact to air pollutant concentrations at the vicinity of the airport. Simulations were performed with the USEPA's Industrial Source Complex Short Term (ISC3-ST) steady-state Gaussian plume model using an emission inventory for the main aircraft engines during the Landing and Take-Off (LTO) cycle, APU's and handling equipment.

The innovative character of this study lies in the construction of a near real time (hourly) emission inventory of Copenhagen airport with a simultaneous quantification of airport emissions of NO_x, CO, PM and UFPs in the nearby area. Evaluating human exposure arising from airport emissions is an important scientific result to highlight the corresponding potential human health impact and possible mitigating measures.

2. Material and Methods

2.1. Study Area

The current study focuses on the estimation of CO, NO_x, PM and PN emissions and corresponding ground level concentrations at Copenhagen airport, Denmark. The Copenhagen airport (CPH) is located at Kastrup in Denmark and flight traffic was recorded during a week in the cold period (March 2025). Average weekly traffic (arrivals and departures) for this period was 4295 flights. Increased flight traffic (5283 flights) during a warm period in July 2025 showed a 23% increase in comparison to the cold season. A detailed emission inventory was produced for aircraft main engines, Auxiliary Power Units (APU's) and handling equipment.

2.2. Emissions from Main Engines

Emissions from main engines were calculated for five discrete aircraft phases: taxi-out, take off, climb-out, approach/landing and taxi-in. The aviation LTO emissions calculator provided by the European Environment Agency (EEA) [23] was used for estimating CO, NO_x and PM emissions. Specifically, an excel-based tool was used for estimating the pollutant mass (kg) emitted by aircrafts during the LTO cycle. Input data included the aircraft type, the airport and the study year [23]. Emission estimations were performed by corresponding each aircraft type with the respective engine model following ICAO guidelines [24,25]. Since, the emission calculator provided by EEA, which is based on ICAO database, did not account for PN emissions an alternative methodology was used based on Kinsey et al. [26].

Emissions (E_i) have been calculated incorporating the total activity of all different aircraft types in the airport under study [24,25]:

$$E_i = \sum_{j=1}^m A_j \times \sum_{k=1}^p TIM_{jk} \times FF_{jk} \times Ei_{ijk} \times Ne_j \quad (1)$$

where, E_i is the total emission of pollutant i produced by all aircraft types [g], j is the aircraft type, m are the total number of aircraft types operated in the airport, k is the LTO mode (approach/landing, taxi-in, taxi-out, take-off, climb out), p is the total number of LTO modes (i.e., five), A_j is the total activity of aircraft type j [LTO's], TIM_{jk} is the time-in-mode for mode k for aircraft type j [s], FF_{jk} is the fuel flow for mode k for each engine used on aircraft type j [kg/s], Ei_{ijk} is the emission index for pollutant i in mode k for engine used on aircraft type j [g/kg of fuel], Ne_j is the number of engines used on aircraft type j .

The emission rates have been evaluated using the whole LTO cycle, the duration and the source area of the different LTO modes. The emission rates are given as:

$$Er_i = \frac{\sum_{j=1}^m A_j \times TIM_{jk} \times FF_{jk} \times Ei_{ijk} \times Ne_j}{E_t \times E_s} \quad (2)$$

where Er_i is the emission rate of pollutant i produced by all aircraft types during LTO mode k [g/(s·m²)], E_t is the total time of studied period [s] and E_s is the emission source area [m²].

According to Kinsey et al. [26], the PN emission index decreases as fuel flow rate increases based on the Engine Exhaust particle sizer (EEPS) data. The number of particles per kg of fuel burnt was estimated with Equation (3) [7,26]:

$$El_n = m \times \ln(\text{fuel}_{flow}) + b \quad (3)$$

where fuel_{flow} is the engine fuel consumption (kg/h), the constants m and b were set equal to (-2) and (2×10^{17}) , respectively.

The PN emissions (particles) was estimated by Equation (4):

$$PN_{emissions} = El_n \times m_{fb} \quad (4)$$

where m_{fb} is the mass (kg) of fuel burnt and was derived from the aviation LTO emissions calculator provided by the EEA (2023). Particles considered to be in the size range of 10–30 nm thus coagulation is the dominant mechanism for the initial particle emissions [27]. The theory of particle coagulation states that the half time is dependent on the initial particle number concentration and equal to 20 s for an initial number concentration of 10^8 particles/cm³ [27].

In the current work all airplanes grouped into three size categories: small, medium, and large. A representative aircraft model was selected for each category to serve as the basis for emission calculations: Small aircraft: Learjet 45 (LJ45) equipped with TFE731-20AR-1B engines; Medium aircraft: Airbus A320neo; Large aircraft: Airbus A330-300 (A333) equipped with Rolls-Royce Trent 772 engines. Moreover, engine technical characteristics such as smoke number (SN), bypass ratio (BPR) [28] and air to fuel ratio (AFR) [25] were used for the calculations [7]. A first order approximation version 3 (FOA3) method was used for estimating the PM emission factors. Based on FOA3, the non-volatile PM is dependent on engine technical characteristics such as SN, BPR and AFR. Specifically, the non-volatile PM (EI_{PMnvol} ; mg/kg fuel) was estimated by [24]:

$$EI_{PMnvol} = CI \times Q \quad (5)$$

where CI is the carbon index (mg/m³) and Q is the exhaust volumetric flow (m³/kg). The CI and Q were estimated by the following equations [24]:

$$CI = 0.06949 \times (SN)^{1.234} \quad \text{for } SN \leq 30 \quad (6)$$

$$CI = 0.0297 \times (SN)^2 - 1.803 \times (SN) + 31.94 \quad \text{for } SN > 30 \quad (7)$$

$$Q = 0.776 \times (AFR) + 0.877 \quad \text{for core engine} \quad (8)$$

$$Q = 0.7769 \times (AFR) \times (1 + BPR) + 0.877 \quad \text{for mixed flow} \quad (9)$$

The SN is dependent on the LTO mode and the type of aircraft engine, and ranged from 0.2 to 1.8 for Rolls-Royce Trent 772 engines. The BPR is dependent on the type of aircraft engine and was equal to 5.2 for Rolls-Royce Trent 772 engines. These values derived from ICAO engine exhaust emission data sheet from ICAO Aircraft Engine Emissions Databank. The AFR is dependent on the LTO mode and ranged from 45 to 106 [24].

2.3. Auxiliary Power Units (APUs) and Handling Emissions

The emissions from APUs were estimated following the methodology by the International Civil Aviation Organization [25]. ICAO categorized the aircrafts into two operational groups: short-haul aircraft (which includes small and medium aircrafts) and long-haul aircraft (large aircraft). The APU emissions for each aircraft operation are presented in Table 1.

Table 1. APU emissions for each aircraft operation [25].

	Short-Haul	Long Haul
NO _x (g)	700	2400
CO (g)	310	210
PM (g)	40	50
PN (#)	5.75×10^{17}	3.75×10^{17}

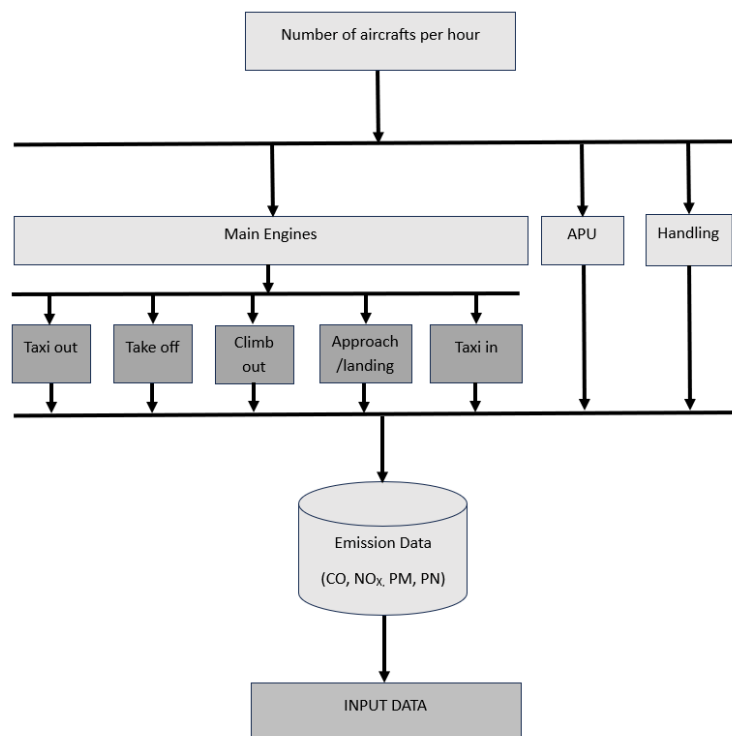
The handling emissions were also estimated using the methodology of the International Civil Aviation Organization [25]. According to the ICAO [25], handling sources include ground support equipment (GSE) and other sources such as aircraft fueling and airside vehicles. The Handling emissions are presented in Table 2.

Table 2. Handling equipment emissions for narrow and wide-body aircraft [25].

	Narrow-Body Aircraft	Wide-Body Aircraft
NO _x (kg/cycle)	0.260	0.510
CO (kg/cycle)	0.100	0.225
PM (kg/cycle)	0.015	0.030
PN (#cycle)	4.0×10^{13}	1.1×10^{14}

The emissions in Table 2 represent a full flight cycle (including both arrival and departure), the results divided by two to avoid double counting and ensure that each operation was only accounted once. This approach allowed to estimate the emissions generated by various ground support equipments, such as baggage loaders, pushback tractors, and catering trucks, during aircraft turnaround operations.

The technical implementation of the airport emissions is presented in Figure 1. The aircraft activity (aircrafts h⁻¹) in the present study refers exclusively to civil aviation aircraft movements. The taxi-in, taxi-out, and take-off phases were considered as ground-level operations. The approach and landing phases occur at horizontal distances until the aircraft reduces its altitude from 3000 ft. to ground-level or reaches the altitude of 3000 ft. after take-off. Overall, emissions from aircraft engines are closely tied to the airport's busiest hours, particularly during morning and midday flight activity. The aircraft main engines are the largest contributors to CO, NO_x, and particle number emissions. These emissions are primarily generated during phases such as taxiing, take-off, and climb-out. However, the Auxiliary Power Units (APUs) is the dominant source to particle mass and contribute to the NO_x emissions.

**Figure 1.** Flow chart with technical implementation of the aircraft emission flow estimator.

2.4. Dispersion Model

The atmospheric dispersion ISC3-ST model [29] was used for the estimation of CO, NO_x, PM and PN concentrations. The ISC3-ST model was adopted due to the operational simplicity and the smaller amounts of meteorological data required in comparison with the AERMOD model [30]. The ISC3-ST is a steady-state Gaussian plume model for modelling air pollutants concentration from point, area, volume and open-pit sources. In the ISC3-ST model line sources are not available and emissions are modeled as area or volume sources. Although AERMOD includes line sources for on-road traffic sources, area sources are still recommended by several studies as the preferred method for representing aircraft emissions [20]. The use of area sources to represent the LTO cycle is a well-established approach and has been used in several other studies [7,18–20].

Input data required for the implementation of the ISC3-ST model includes meteorological data and source emission characteristics. The meteorological data were derived from a weather underground site [31] which has historical data from Copenhagen Kastrup airport station. The hourly meteorological data are presented in Figure 2. The release height of emission sources which refer to take-off, taxi-in and taxi-out was set equal to 2 m while the release height of emission sources which refer to climb out and approach/landing was set equal to 1500 ft (457.2 m) [7]. The release height of APUs and handling equipments emissions were set equal to 0.5 m. Additionally, the receptor height was set equal to 1.5 m which corresponds to the typical human receptor breathing zone height.

A limitation of the current study is that using a model such as the ISC3-ST may lead to different concentrations predictions and may overestimate the air pollutants concentrations compared to AERMOD model. Another limitation of the current work is that area sources in ISC3-ST model assume that the pollutants are released at a fixed height and ignore plume rise from buoyant exhausts. The Gaussian dispersion models are highly sensitive to meteorological inputs. Rao et al. [32] asserted that air pollutant concentrations cannot be predicted accurately with meteorological data uncertainties affecting the precision of estimated concentrations levels.

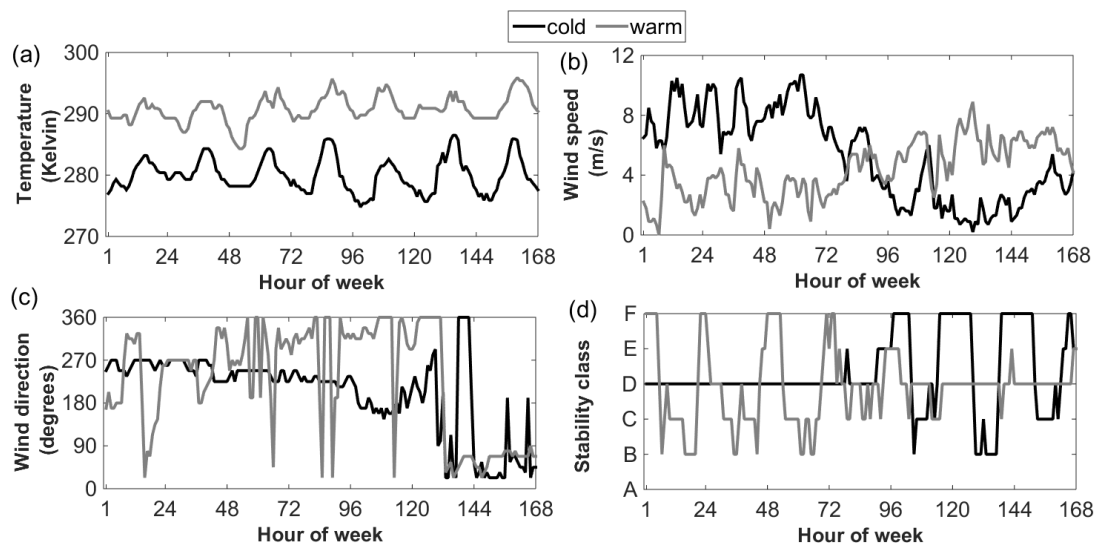


Figure 2. Hourly meteorological data ((a) temperature (Kelvin), (b) wind speed (m/s), (c) wind direction(degrees), (d) stability class) in the Copenhagen airport during cold (3–9 March 2025) and warm (7–13 July 2025) period.

2.5. Traffic Data

The average aircraft activity (aircrafts h^{-1}) for a week at CPH during the cold period of 2025 is shown in Figure 3. Overall, flight activity was higher on Monday, especially during the morning hours. There is a clear morning peak around 8:00 a.m. on Monday, particularly for departures, reflecting typical weekday business travel patterns. In contrast, Saturday shows a more balanced and steady flight distribution throughout the day, with a less pronounced morning peak. Moreover, a general pattern of increased activity during the daytime and reduced activity at night was observed during the whole week. Private aircrafts have not been included in this study. The commercial aircraft activity has been analyzed according to the Landing and Take-Off (LTO) cycle which includes five discrete aircraft phases: (1) approach below 3000 ft. and landing, (2) arrival (taxi-in) to the parking area, (3) departure (taxi-out) from the parking area, (4) take-off, and (5) climb out up to 3000 ft. [25,28].

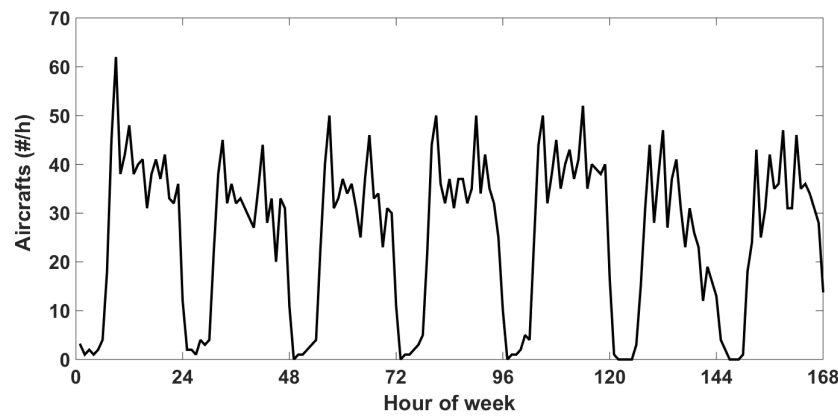


Figure 3. Number (#) of aircrafts per hour during a week in the cold period of 2025 at Copenhagen airport.

3. Results and Discussion

3.1. Air Pollutant (CO , NO_x , PM and PN) Emissions at the Copenhagen Airport

Figure 4 shows the average hourly CO emissions (kg) during the cold period from different sources. CO has been mostly released during taxi-in and taxi-out phases. CO emissions are highest during the early morning hours, with a sharp peak around 08:00. This increase is primarily driven by the taxi-out phase, which is the dominant contributor to the total CO output. APUs have also a contribution to the overall CO emissions with a smaller contribution from landing [33].

NO_x emissions (Figure 5) follow a similar time pattern but differ in their source since the climb-out phase is the main contributor to overall NO_x emissions [33]. The NO_x levels show two clear peaks, one in the morning and another around early afternoon, reflecting the airport's peak operational periods. The NO_x emissions are higher during approach/landing, take-off and climb out compared to those during taxi-in and taxi-out. During take-off and above-the-ground phases, engines receive larger amounts of air which results to increased AFR and higher amounts of nitrogen (N_2) during combustion [33].

PM and PN emissions (Figures 6 and 7) show a similar daily distribution. The climb-out and taxi-out phases account for the majority of emissions. Overall, emissions from aircraft engines are closely tied to the airport's busiest hours, particularly during morning and midday flight activity. The aircraft main engines are the largest contributors to CO , NO_x , and particle number emissions. These emissions are primarily generated during phases such as taxiing, take-off, and climb-out. However, the Auxiliary Power Units (APUs) is the dominant source to particle mass (Figure 6) and contribute to the NO_x emissions (Figure 5).

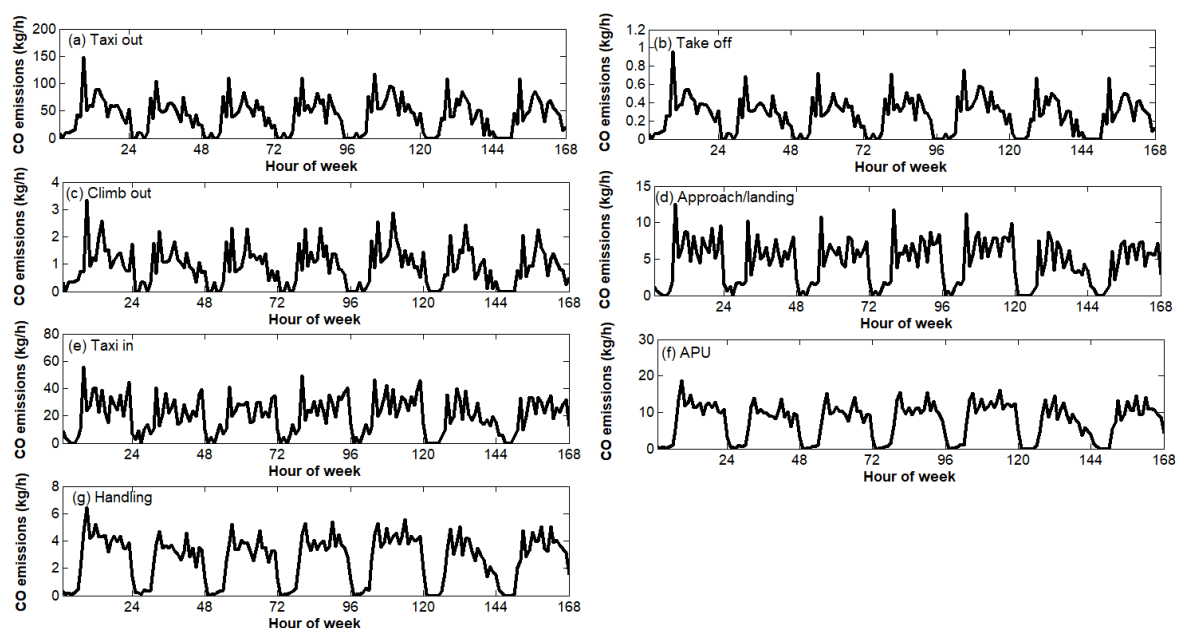


Figure 4. Hourly CO emissions (kg) during a week of the cold period and under different sources ((a) taxi out, (b) take off, (c) climb out, (d) approach/landing, (e) taxi in, (f) APU, (g) handling) at Copenhagen airport.

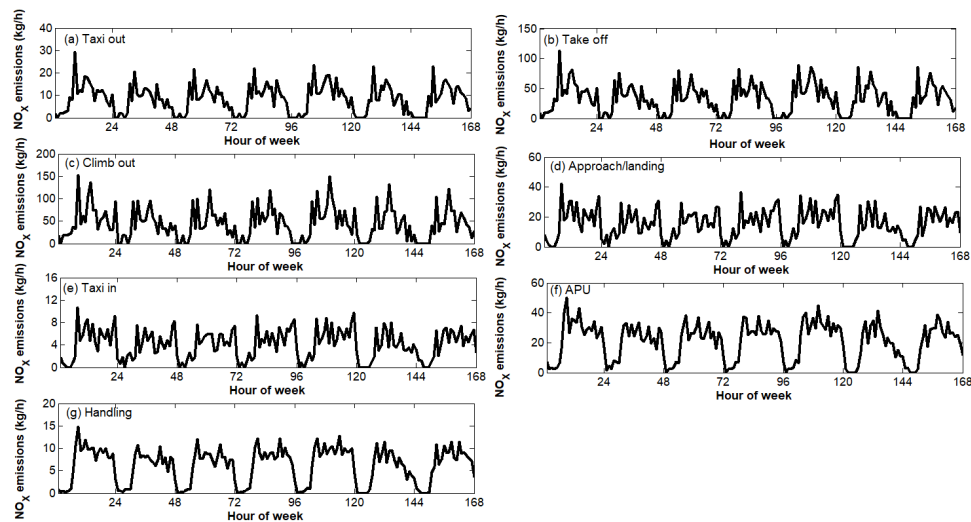


Figure 5. Hourly NO_x emissions (kg) during a week of the cold period and under different sources ((a) taxi out, (b) take off, (c) climb out, (d) approach/landing, (e) taxi in, (f) APU, (g) handling) at Copenhagen airport.

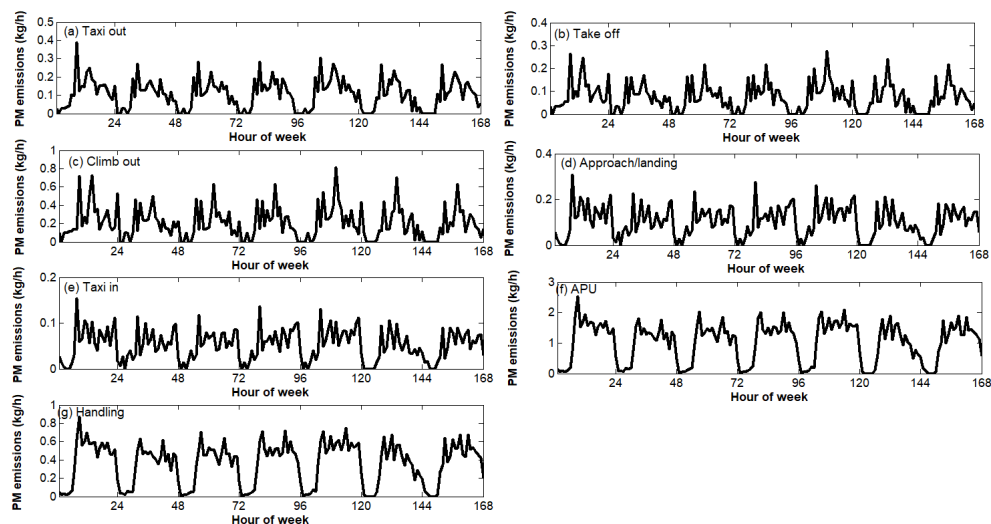


Figure 6. Hourly PM emissions (kg) during a week of the cold period and under different sources ((a) taxi out, (b) take off, (c) climb out, (d) approach/landing, (e) taxi in, (f) APU, (g) handling) at Copenhagen airport.

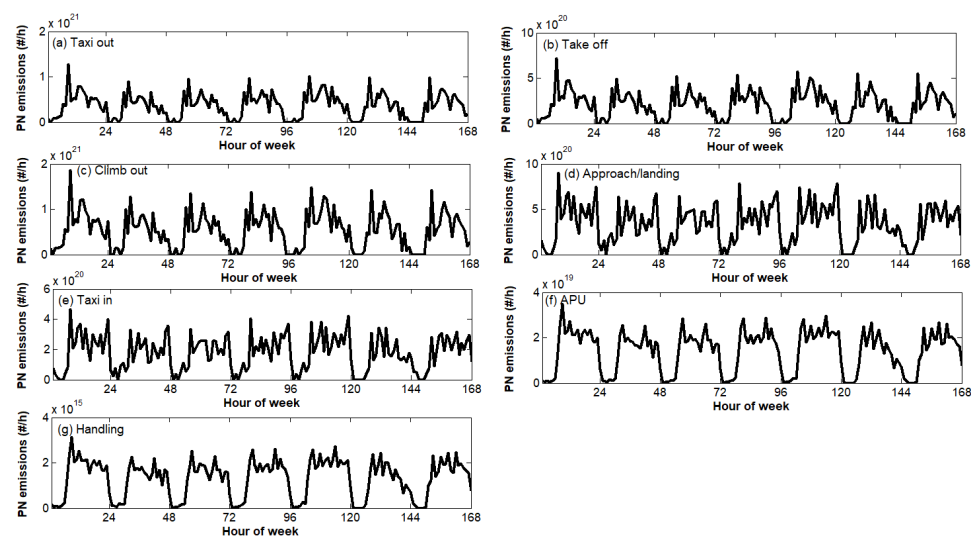


Figure 7. Hourly PN emissions (#/h) during a week of the cold period and under different sources ((a) taxi out, (b) take off, (c) climb out, (d) approach/landing, (e) taxi in, (f) APU, (g) handling) at Copenhagen airport.

Table 3 summarizes the weekly emissions of air pollutants from the Copenhagen airport during different airport activities during the cold period of 2025. The LTO cycle is contributing mainly to PN, NO_x and CO emissions. Contrary APU emissions contribute mainly to PM and NO_x emissions. Figure 8 shows also the contribution percentage of the different airport activities to air pollutant emissions. Taxi out is a main contributor to CO and PN emissions and emits close to 53% of CO and 22% of PN. Climb out and landing are also main contributors to PN (53%) and NO_x (45%). APU also contributes to 53% of PM mass and 10% of NO_x emissions. Taxi in is also responsible for 11% of PN and 26% of CO emissions.

Moreover, calculations for the whole year 2025 were estimated by summing the daily emissions during both periods (cold and warm) and where equal to 759,393 kg for CO, 1,285,387 kg for NO_x, 19,013 kg total for PM and 1.6×10^{25} for fine particles.

Table 3. Weekly emissions of air pollutants (CO, NO_x, PM, PN) at Copenhagen airport during the cold period.

	CO kg/Week	NO _x kg/Week	PM kg/Week	PN #/Week
Taxi out	6970	1411	18	6.1×10^{22}
Take off	44	5514	13	3.5×10^{22}
Climb out	153	7421	35	9.0×10^{22}
Approach/landing	765	2570	17	5.7×10^{22}
Taxi in	3407	689	9	3.0×10^{22}
APU	1299	3554	175	2.4×10^{21}
Handling	459	1047	62	2.2×10^{17}

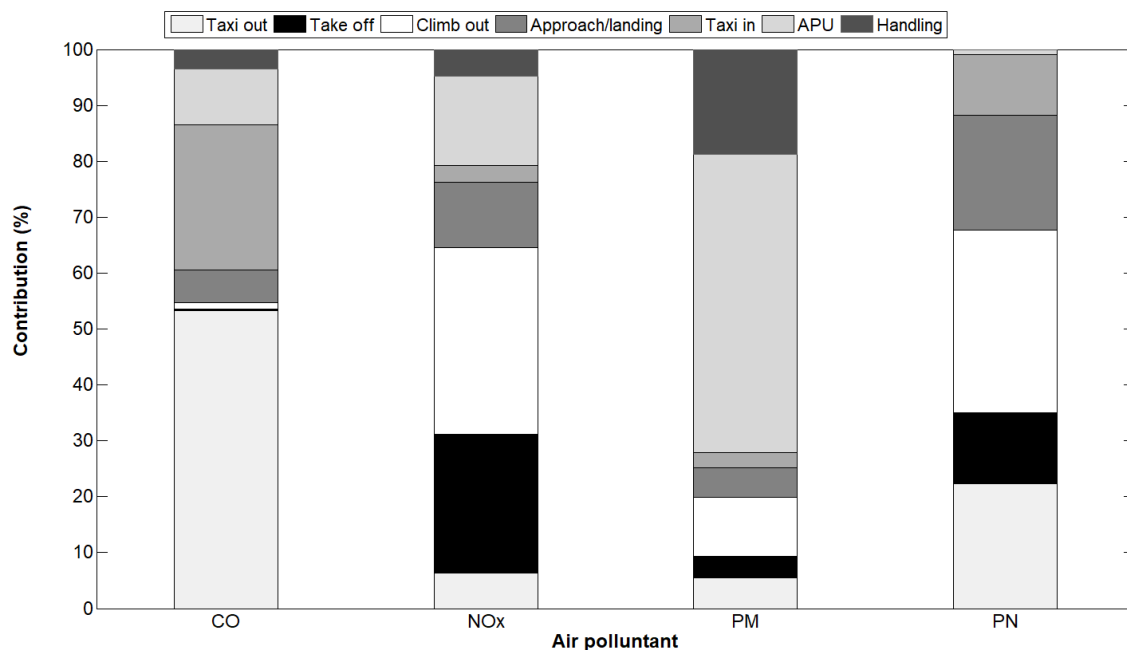


Figure 8. Contribution of each aircraft activity to CO, NO_x, PM and PN emissions at Copenhagen airport.

3.2. Daily CO and NO_x Concentration Distribution

Simulations were performed for a day characterized by highest aircraft activity and meteorological conditions that favored transport of air masses to the direction towards the city. Ground based daily CO concentration levels arising from the airport activities during Friday 7 March are presented in Figure 9. Friday was a day with the highest aircraft activity during the week both during the cold and warm period. Concerning CO, simulations indicated accumulation at the northern area of the airport around the aircraft's parking area and at the end of runway with highest value close to 3000 $\mu\text{g}/\text{m}^3$. Concentrations of 20 $\mu\text{g}/\text{m}^3$ can reach neighboring residential areas at distances of 5 km north following the wind profile (see Figure 9b). CO concentrations were found considerably lower than the maximum regulated 8-hour average value of 10,000 $\mu\text{g}/\text{m}^3$. Although CO emissions are below health risk thresholds, the chronic low-level exposure can lead to significant health effects for workers at airports. Savioli et al. [34] reported that chronic low-level exposure to CO in professional setting causes neurological syndromes (headache, dizziness, nausea). Herein, CO concentrations reached 3000 $\mu\text{g}/\text{m}^3$ at the

parking area of Copenhagen airport while Kuzu [19] found CO concentration at the parking area of Ataturk international airport (Turkey) much higher at $19,839 \mu\text{g}/\text{m}^3$.

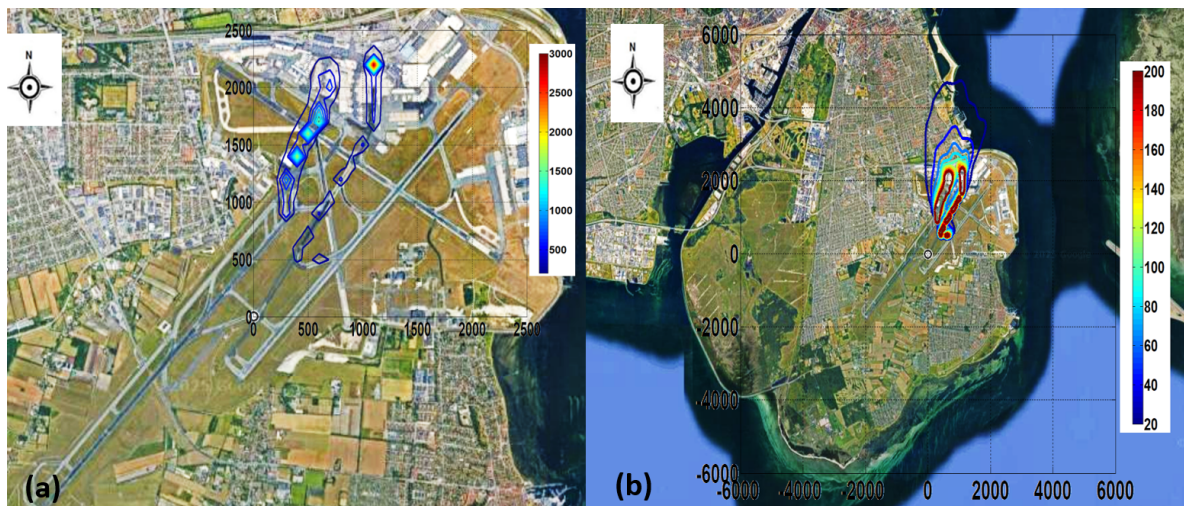


Figure 9. Daily ground based concentration of CO ($\mu\text{g}/\text{m}^3$) on Friday March 7 at Copenhagen airport: (a) $200 \mu\text{g}/\text{m}^3$ to $3000 \mu\text{g}/\text{m}^3$ with level step $200 \mu\text{g}/\text{m}^3$ and (b) $20 \mu\text{g}/\text{m}^3$ to $200 \mu\text{g}/\text{m}^3$ with level step $20 \mu\text{g}/\text{m}^3$.

The ground level daily concentrations of NO_x for Friday 7 March showed elevated concentrations which exceeded the regulated hourly value of $200 \mu\text{g}/\text{m}^3$ near the airfields and the airport area (Figure 10). Nevertheless, NO_x concentration in a zone that expands close to 2 km at the North East of the airport was close to $20 \mu\text{g}/\text{m}^3$. Inside the airport area, especially at the aircraft parking area and the runway, NO_x concentrations reached daily values close to $1000 \mu\text{g}/\text{m}^3$ with a maximum daily value of $7000 \mu\text{g}/\text{m}^3$. The high levels of NO_x concentrations are partly associated with the omission of plume rise, thereby leading to an overestimation of ground-level concentrations.

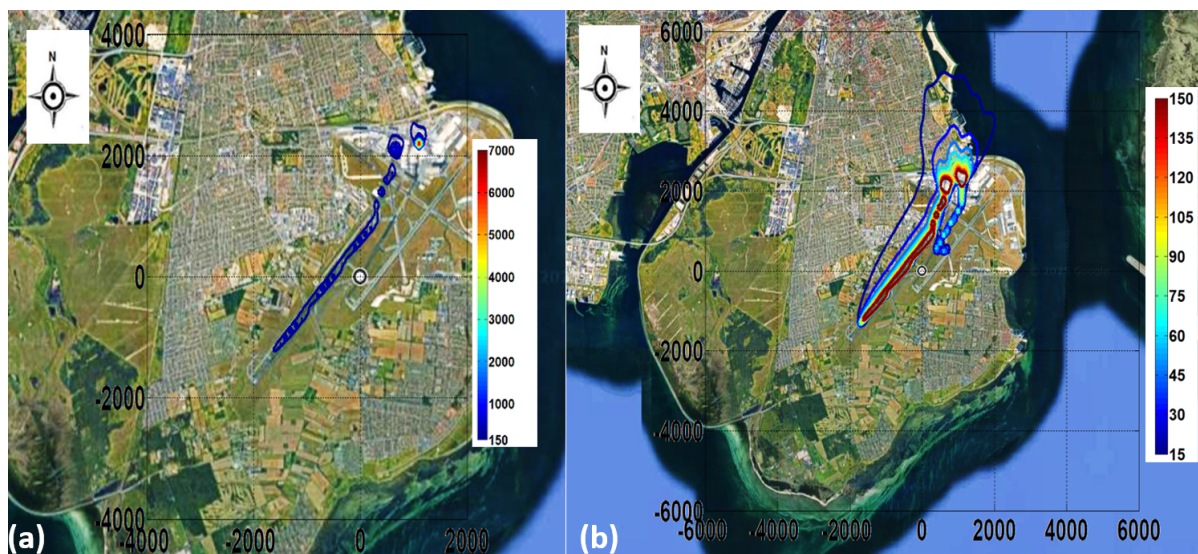


Figure 10. Daily ground based concentration of NO_x ($\mu\text{g}/\text{m}^3$) on Friday 7 March at Copenhagen airport: (a) $150 \mu\text{g}/\text{m}^3$ to $7000 \mu\text{g}/\text{m}^3$ with level step $150 \mu\text{g}/\text{m}^3$ and (b) $15 \mu\text{g}/\text{m}^3$ to $150 \mu\text{g}/\text{m}^3$ with level step $15 \mu\text{g}/\text{m}^3$.

Targeted simulation for NO_x on Friday 7 of March at 18:00 where aircraft activity was the maximum, shows that the hourly threshold was exceeded mainly in the vicinity and inside the airport area (Figure 11). Although NO_x concentrations outside the airport boundary are below health risks threshold, NO_x levels at $20 \mu\text{g}/\text{m}^3$ at the neighboring residential areas is critical and highlight that the airport activities affect the broader regional air quality.

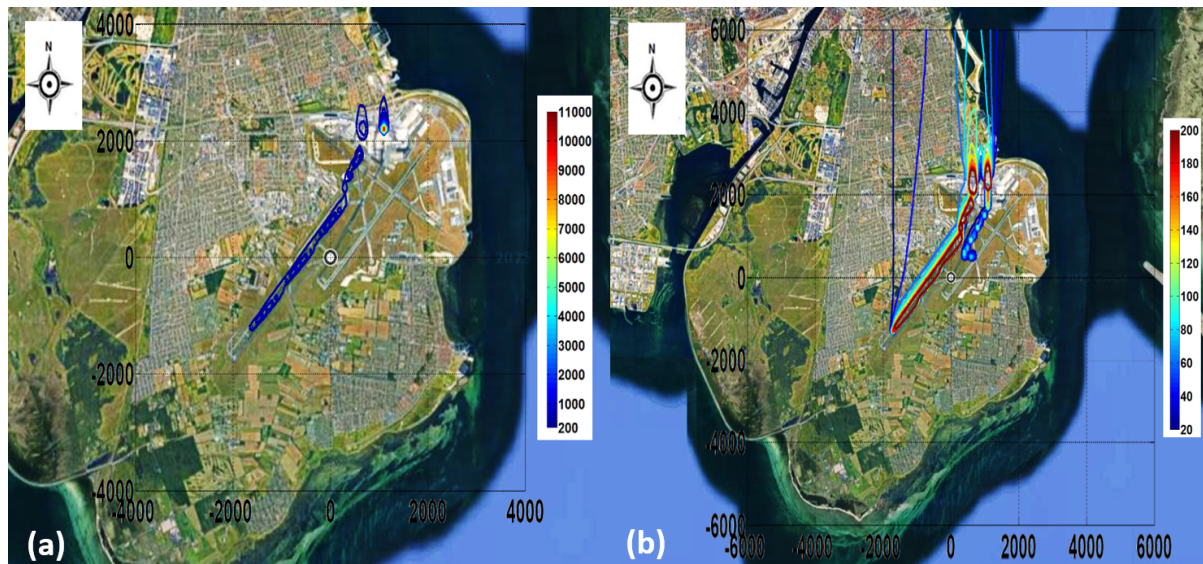


Figure 11. Hourly concentration of NO_x ($\mu\text{g}/\text{m}^3$) on Friday 7 March at Copenhagen airport (18:00): (a) $200 \mu\text{g}/\text{m}^3$ to $11,000 \mu\text{g}/\text{m}^3$ with level step $200 \mu\text{g}/\text{m}^3$ and (b) $20 \mu\text{g}/\text{m}^3$ to $200 \mu\text{g}/\text{m}^3$ with level step $20 \mu\text{g}/\text{m}^3$.

3.3. Daily PM and PN Concentration Distribution

Daily PM concentration ($\mu\text{g}/\text{m}^3$) are affected mainly from APUs and as shown in Figure 12 elevated concentrations occur very close to the sources inside the airport area. This indicates that impact from exposure to PM is primary an on-site occupational/worker concern rather than a long-range dispersion issue. Herein, PM concentrations were higher ($\approx 350 \mu\text{g}/\text{m}^3$) than those found in an airport in Italy where the maximum daily concentration was less than $12.5 \mu\text{g}/\text{m}^3$ [18]. Daily concentrations up to $1 \mu\text{g}/\text{m}^3$ may occur at distances 2 km north from the airport.

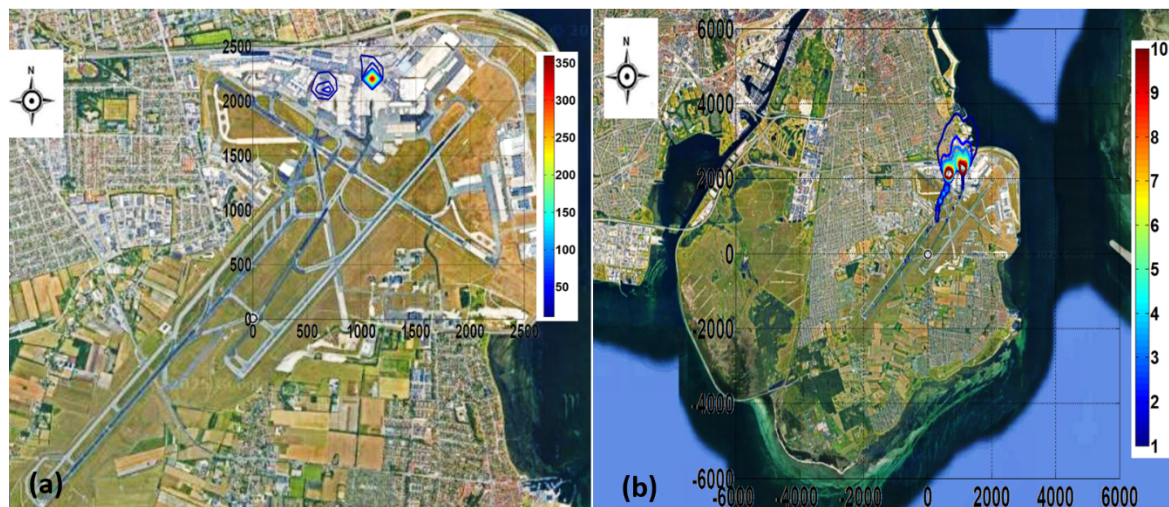


Figure 12. Daily concentration of PM ($\mu\text{g}/\text{m}^3$) on Friday 7 March at Copenhagen airport: (a) $10 \mu\text{g}/\text{m}^3$ to $350 \mu\text{g}/\text{m}^3$ with level step $10 \mu\text{g}/\text{m}^3$ and (b) $1 \mu\text{g}/\text{m}^3$ to $10 \mu\text{g}/\text{m}^3$ with level step $1 \mu\text{g}/\text{m}^3$.

Daily average PN concentration as high as $100,000$ particles/ cm^3 were estimated at the parking area and the main runway whereas values close to $10,000$ particles/ cm^3 were estimated overall at the airport (Figure 13a). The great variation in the levels of PN within the airport reflects the rapid dilution and decay of UFPs, which is significantly driven by coagulation. Average daily average concentrations of 1000 particles/ cm^3 at distances close to 1 km from emissions sources indicated particles transport in the vicinity of the airport (Figure 13b).

Aircraft takeoffs contributed to elevated concentrations of ultrafine particles up to 10^7 particles per cm^3 [15] at the Los Angeles International airport. Concentrations of ultrafine particles up to $800,000$ particles per cm^3 were also observed at the Mytilini airport [35].

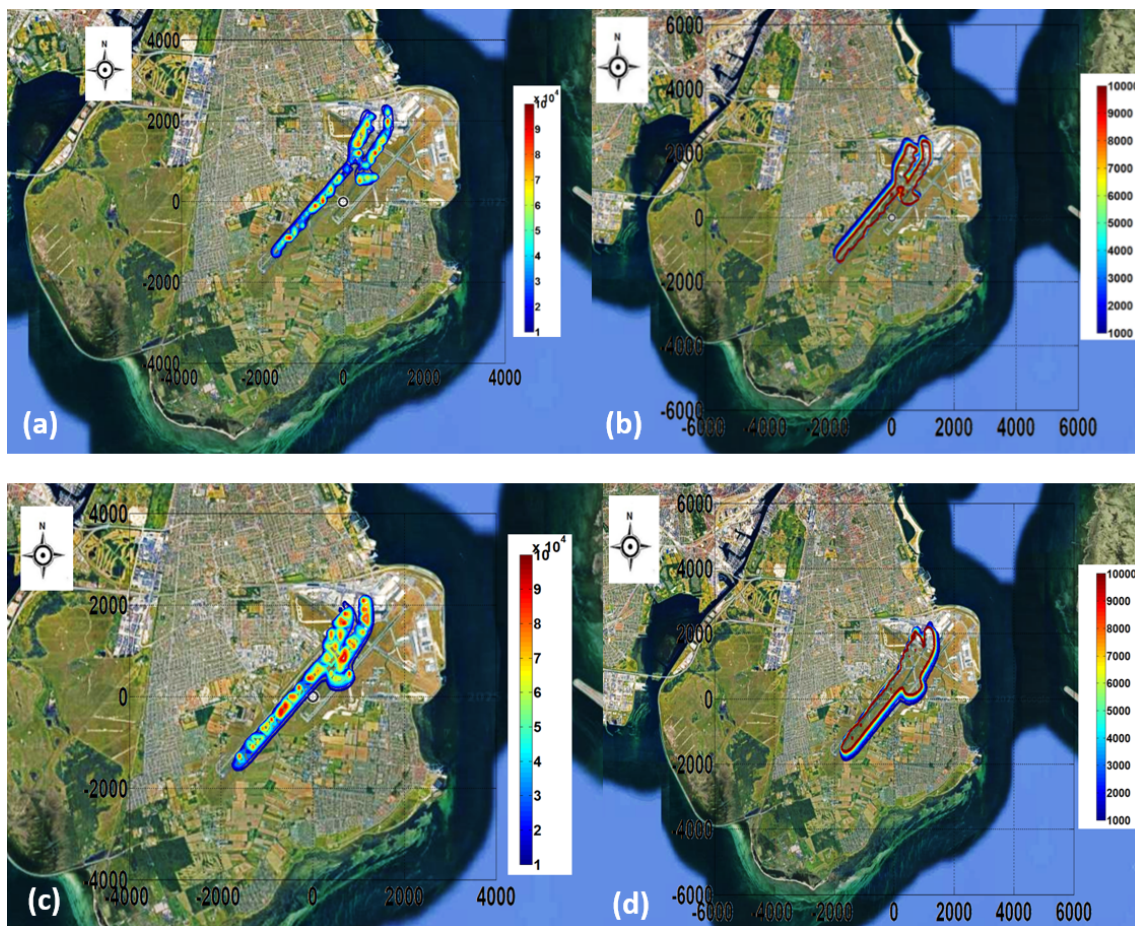


Figure 13. Daily concentration of PN (#/cm³) on Friday 7 March 2025 at Copenhagen airport: (a) 10,000 #/cm³ to 100,000 #/cm³ with level step 10,000 #/cm³ (cold period, Friday 7 March 2025), (b) 1000 #/cm³ to 10,000 #/cm³ with level step 1000 #/cm³ (cold period, Friday 7 March 2025), (c) 10,000 #/cm³ to 100,000 #/cm³ with level step 10,000 #/cm³ (warm period, Friday 11 July 2025) and (d) 1000 #/cm³ to 10,000 #/cm³ with level step 1000 #/cm³ (warm period, Friday 11 July 2025).

A comparison between the cold and warm period for the day with the maximum number of flight is shown in Figure 13. A specific day was chosen due to the meteorological conditions that favored transport of air masses towards the city. Accordingly, PN emissions during the warm period were higher by 23% than during the cold period. Daily number concentration was equal to 1640 particles/cm³ during the cold period and 2282 particles/cm³ during the warm period as estimated at a distance of 1 km in the east and 2.5 km in the north from the Copenhagen airport (55.607893, 12.635043). Lower concentrations were observed on Saturdays.

Weather stability class under different seasons may also affect pollutant concentration levels since stable conditions prevail during the cold period, while neutral conditions occur more often during the warm period. Air pollutant concentration under stable conditions are higher compared to neutral conditions [36].

4. Conclusions

Emissions and dispersion of air pollutants from LTO cycle of aircrafts, APUs and handling equipment at the Copenhagen airport were simulated using the ISC3-ST model on selected weeks during 2025. Two periods, a cold and a warm one were evaluated with increased traffic by 23% during the warm period. Emissions followed the daily flight activity, with distinct peaks during morning and midday hours, particularly on weekdays. Aircraft main engines were the largest contributors to CO, NO_x, and PN emissions within the airport area. Auxiliary Power Units (APUs) and ground handling equipment contributed mainly to PM emissions. Model simulations revealed that the contribution from airport activities to the ground level concentration of CO and PM was not significant in the vicinity of the airport. However, aircraft main engines contributed significantly to the local air quality levels of NO_x and PN at the airport facilities and in the vicinity of the airport.

The aircraft LTO cycle contributed largely to ambient NO_x and PN concentrations inside the airport a finding that constitutes exposure particularly important for the personnel and travelers. In addition, dispersion simulations

underlined pollutant transport to nearby areas, therefore affecting directly human exposure and populations living close to the airport.

This work highlights the need for emissions reduction at airport facilities by adopting targeted and environmentally friendly measures. Detailed emission profiling is necessary for more effective airport environmental management. Reducing emissions from APUs and ground handling vehicles presents a tangible opportunity to improve air quality in respect to particle mass without compromising operations.

Author Contributions

M.L.: conceptualization, methodology, supervision, funding acquisition, writing—review & editing, E.C.: methodology, review & editing, M.B.: investigation, data curation, methodology, P.G.: investigation, data curation, methodology, S.E.C.: review & editing. All authors have read and agreed to the published version of the manuscript.

Funding

The authors gratefully acknowledge the financial support of the European Commission under grant MI-TRAP, which was funded from the H2020 RTD Framework Program of the European Union (Grant agreement no: 101138449).

Institutional Review Board Statement

Not applicable.

Informed Consent Statement

Not applicable.

Data Availability Statement

The datasets generated during the current study are available from the corresponding author (lazaridi@mred.tuc.gr) on reasonable request.

Conflicts of Interest

The authors declare no conflict of interest. Given the role as a member of the Editorial Board, Mihalis Lazaridis had no involvement in the peer review of this paper and had no access to information regarding its peer-review process. Full responsibility for the editorial process of this paper was delegated to another editor of the journal.

Use of AI and AI-Assisted Technologies

No AI tools were utilized for this paper.

References

1. Pope, C.A.; Ezzati, M.; Dockery, D.W. Fine Particulate Air Pollution and Life Expectancy in the United States. *N. Engl. J. Med.* **2009**, *360*, 376–386. <https://doi.org/10.1056/nejmsa0805646>.
2. World Health Organization (WHO). *WHO Air Quality Guidelines for Particulate Matter, Ozone, Nitrogen Dioxide and Sulfur Dioxide*; WHO Press: Geneva, Switzerland, 2021; pp 1–290.
3. Gruzieva, O.; Jeong, A.; He, S.; et al. Air Pollution, Metabolites and Respiratory Health across the Life-Course. *Eur. Respir. Rev.* **2022**, *31*, 220038. <https://doi.org/10.1183/16000617.0038-2022>.
4. Avogadro, N.; Redondi, R. Pathways toward Sustainable Aviation: Analyzing Emissions from Air Operations in Europe to Support Policy Initiatives. *Transp. Res. Part A Policy Prac.* **2024**, *186*, 104121. <https://doi.org/10.1016/j.tra.2024.104121>.
5. Masiol, M.; Harrison, R.M. Aircraft Engine Exhaust Emissions and Other Airport-Related Contributions to Ambient Air Pollution: A Review. *Atmos. Environ.* **2014**, *95*, 409–455. <https://doi.org/10.1016/j.atmosenv.2014.05.070>.
6. Winther, M.; Uffe, K.; Thomas, E.; et al. Emissions of NO_x, Particle Mass and Particle Numbers from Aircraft Main Engines, APU's and Handling Equipment at Copenhagen Airport. *Atmos. Environ.* **2015**, *100*, 218–229. <https://doi.org/10.1016/j.atmosenv.2014.10.045>.

7. Makridis, M.; Lazaridis, M. Dispersion Modeling of Gaseous and Particulate Matter Emissions from Aircraft Activity at Chania Airport, Greece. *Air Qual. Atmos. Health* **2019**, *12*, 933–943. <https://doi.org/10.1007/s11869-019-00710-y>.
8. Pandey, G.; Venkatram, A.; Arunachalam, S. Modeling the Air Quality Impact of Aircraft Emissions: Is Area or Volume the Appropriate Source Characterization in AERMOD? *Air Qual. Atmos. Health* **2024**, *17*, 1425–1434. <https://doi.org/10.1007/s11869-024-01517-2>.
9. Yang, J.; Li, L.; Zheng, X.; et al. Pollutants Dispersion of Aircraft Exhaust Gas During the Landing and Takeoff Cycle with Improved Gaussian Diffusion Model. *Atmosphere* **2024**, *15*, 1256. <https://doi.org/10.3390/atmos15101256>.
10. Riley, K.; Cook, R.; Carr, E.; et al. A Systematic Review of the Impact of Commercial Aircraft Activity on Air Quality Near Airports. *City Environ. Interact.* **2021**, *11*, 100066. <https://doi.org/10.1016/j.cacint.2021.100066>.
11. Dissanayaka, M.; Ryley, T.; Spasojevic, B.; et al. Modeling Aircraft Emissions during the Taxiing to Assess Air Quality Impacts: An Australian Airport Case Study. *J. Air Transp. Manag.* **2026**, *131*, 102918. <https://doi.org/10.1016/j.jairtraman.2025.102918>.
12. Alzahrani, S.; Kilic, D.; Flynn, M.; et al. International Airport Emissions and Their Impact on Local Air Quality: Chemical Speciation of Ambient Aerosols at Madrid–Barajas Airport during the aviator Campaign. *Atmos. Chem. Phys.* **2024**, *24*, 9045–9058. <https://doi.org/10.5194/acp-24-9045-2024>.
13. Carslaw, D.C.; Beevers, S.D.; Ropkins, K.; et al. Detecting and Quantifying Aircraft and Other On-Airport Contributions to Ambient Nitrogen Oxides in the Vicinity of a Large International Airport. *Atmos. Environ.* **2006**, *40*, 5424–5434. <https://doi.org/10.1016/j.atmosenv.2006.04.062>.
14. Yang, X.; Cheng, S.; Lang, J.; et al. Characterization of Aircraft Emissions and Air Quality Impacts of an International Airport. *J. Environ. Sci.* **2018**, *72*, 198–207. <https://doi.org/10.1016/j.jes.2018.01.007>.
15. Zhu, Y.; Fanning, E.; Yu, R.C.; et al. Aircraft Emissions and Local Air Quality Impacts from Takeoff Activities at a large International Airport. *Atmos. Environ.* **2011**, *45*, 6526–6533. <https://doi.org/10.1016/j.atmosenv.2011.08.062>.
16. Pecorari, E.; Mantovani, A.; Franceschini, G.; et al. Analysis of the Effects of Meteorology on Aircraft Exhaust Dispersion and Deposition Using a Lagrangian Particle Model. *Sci. Total Environ.* **2016**, *541*, 839–856. <https://doi.org/10.1016/j.scitotenv.2015.08.147>.
17. Yim, S.H.L.; Lee, G.L.; Lee, I.H.; et al. Global, Regional and Local Health Impacts of Civil Aviation Emissions. *Environ. Res. Lett.* **2015**, *10*, 034001. <https://doi.org/10.1088/1748-9326/10/3/034001>.
18. Simonetti, I.; Maltagliati, S.; Manfrida, G. Air Quality Impact of a Middle Size Airport Within an Urban Context Through EDMS Simulation. *Transp. Res. Part D Transp. Environ.* **2015**, *40*, 144–154. <https://doi.org/10.1016/j.trd.2015.07.008>.
19. Kuzu, S.L. Estimation and Dispersion Modeling of Landing and Takeoff (LTO) Cycle Emissions from Atatürk International Airport. *Air Qual. Atmos. Health* **2018**, *11*, 153–161. <https://doi.org/10.1007/s11869-017-0525-5>.
20. Pandey, G.; Venkatram, A.; Arunachalam, S. Evaluating AERMOD with Measurements from a Major U.S. Airport Located on a Shoreline. *Atmos. Environ.* **2023**, *294*, 119506. <https://doi.org/10.1016/j.atmosenv.2022.119506>.
21. Sanajou, K.; Pina, N.; Tchepel, O. Assessing the Impact of Aircraft Emissions on Local Air Quality Under Current and Future Climate Scenarios: A Case Study of Lisbon Airport. *Environ. Monit. Assess.* **2026**, *198*, 63. <https://doi.org/10.1007/s10661-025-14910-w>.
22. Voogt, M.; Zandveld, P.; Erbrink, H.; et al. Assessment of the Applicability of a Model for Aviation-Related Ultrafine Particle Concentrations for Use in Epidemiological Studies. *Atmos. Environ.* **2023**, *309*, 119884. <https://doi.org/10.1016/j.atmosenv.2023.119884>.
23. European Environment Agency. 1.A.3.a Aviation—Annex X—LTO Emissions Calculator—2023. 2023. Available online: <https://www.eea.europa.eu/en/analysis/publications/emep-eea-guidebook-2023/part-b-sectoral-guidance-chapters/1-energy/1-a-combustion/1-a-3-a-aviation>. (accessed on 16 March 2026).
24. ICAO. Document 9889. Airport Air Quality Manual. 2011. Available online: <https://www.icao.int/sites/default/files/sp-files/environmental-protection/Documents/Doc%209889.SGAR.WG2.Initial%20Update.pdf>. (accessed on 16 March 2026).
25. ICAO. Document 9889. Airport Air Quality Manual. 2020. Available online: https://www.icao.int/sites/default/files/2025-04/9889_cons_en.pdf (accessed on 16 March 2026).

26. Kinsey, J.S.; Dong, Y.; Williams, D.C.; et al. Physical Characterization of the Fine Particle Emissions from Commercial Aircraft Engines during the Aircraft Particle Emissions Experiment (APEX) 1-3. *Atmos. Environ.* **2010**, *44*, 2147–2156. <https://doi.org/10.1016/j.atmosenv.2010.02.010>.
27. Hinds, W.C. *Aerosol Technology: Properties, Behavior and Measurements of Airborne Particles*, 2nd ed.; Wiley Interscience: New York, NY, USA, 1999; pp 1–504.
28. ICAO. Environmental Protection: Annex, 16, Vol. II, Aircraft Engine Emissions. 2008. Available online: <https://www.pilot18.com/wp-content/uploads/2017/10/Pilot18.com-ICAO-Annex-16-Volume-2-Aircraft-Engine-Emissions.pdf>. (accessed on 16 March 2026).
29. US-EPA (1995). User’s Guide for the Industrial Source Complex (ISC3) Dispersion Models, Volume II—Description of Model Algorithms, Office of Air Quality Planning and Standards Monitoring, and Analysis Emissions, USEPA -454/B-95-003b. Available online: <https://gaftp.epa.gov/aqmg/SCRAM/models/other/isc3/isc3v2.pdf>. (accessed on 16 March 2026).
30. Hanna, S.R.; Egan, B.A.; Purdum, J.; et al. Evaluation of the ADMS, AERMOD, and ISC3 Dispersion Models with the OPTEX, Duke Forest, Kincaid, Indianapolis and Lovett Field Datasets. *Int. J. Environ. Pollut.* **2001**, *16*, 301–314. <https://doi.org/10.1504/IJEP.2001.000626>.
31. Weather Underground. Available online: <https://www.wunderground.com/history/daily/dk/kastrup/EKCH> (accessed on 16 March 2026).
32. Rao, K.S. Uncertainty Analysis in Atmospheric Dispersion Modeling. *Pure Appl. Geophys.* **2005**, *162*, 1893–1917. <https://doi.org/10.1007/s00024-005-2697-4>.
33. Lieuwen, T.C.; Yang, V. *Gas Turbine Emissions*; Cambridge University Press: Cambridge, England, UK, 2023; pp 1–368.
34. Savioli, G.; Gri, N.; Ceresa, I.F.; et al. Carbon Monoxide Poisoning: From Occupational Health to Emergency Medicine. *J. Clin. Med.* **2024**, *13*, 2466. <https://doi.org/10.3390/jcm13092466>.
35. Psanis, C.E.; Triantafyllou, M.; Giamarelou, M.; et al. Particulate Matter Pollution from Aviation-Related Activity at a Small Airport of the Aegean Sea Insular Region. *Sci. Total Environ.* **2017**, *596*, 187–193. <https://doi.org/10.1016/j.scitotenv.2017.04.078>.
36. Hu, T.; Yoshie, R. Effect of Atmospheric Stability on Air Pollutant Concentration and Its Generalization for Real and Idealized Urban Block Models Based on Field Observation Data and Wind Tunnel Experiments. *J. Wind Eng. Ind. Aerod.* **2020**, *207*, 104380. <https://doi.org/10.1016/j.jweia.2020.104380>.